Theoretical Investigation of the Hydride Transfer from Formate to NAD^+ and the Implications for the Catalytic Mechanism of Formate Dehydrogenase

Birgit Schiøtt, Ya-Jun Zheng,† and Thomas C. Bruice*

Contribution from the Department of Chemistry, University of California at Santa Barbara, Santa Barbara, California 93106

Received March 5, 1998

Abstract: The hydride transfer reaction between formate and NAD^+ has been investigated by using molecular orbital theory in combination with continuum solvation models. The reaction in the gas phase is extremely exothermic due to the instability of the charged reactant species. The calculations reveal that during the hydride transfer the pyridine ring of NAD^+ takes a *quasi*-boat conformation. The nitrogen atom of the pyridine ring remains planar, which is in agreement with the experimentally established ^{15}N kinetic isotope effect (1.004 ± 0.001) of the formate dehydrogenase catalyzed oxidation of formate to carbon dioxide. The computed value at the HF/6-31+G(d,p) level of theory for the ^{15}N kinetic isotope effect is 1.0042. In solution, however, there is a potential energy barrier for the hydride transfer. At the MP2/6-31G(d)//HF/6-31G(d) level of theory the self-consistent reaction field approach gives a barrier height of 9.0 kcal/mol in acetonitrile ($\epsilon = 35.9$). Direct nucleophilic addition of one of the carboxylate oxygens of formate to the pyridine ring of NAD^+ competes with hydride transfer, and this study reveals that this nucleophilic addition is likely to be preferred over the hydride transfer in the gas phase. Thus, the NAD^+-dependent formate dehydrogenase must orient the substrate formate in the active site in such a fashion as to prevent this competing reaction from occurring. According to the recently solved X-ray crystal structure, it is clear that the Arg-284 and Asn-146 are the two critical amino acid residues that hold formate in the productive orientation for hydride transfer.

Introduction

$NAD(P)^+$-dependent dehydrogenases is a large class of enzymes that catalyze transfer of a hydride from the reduced pyridine−nucleotide coenzymes to a variety of substrates.[1] These enzymes catalyze a number of important metabolic processes, and they have been under extensive investigation.[1] Recently, quantum mechanical methods have been used to investigate the mechanistic details of these dehydrogenase reactions.[2−10] The majority of these studies are based on small model reactions. Though it has now become feasible to examine the enzymatic reaction by employing a hybrid quantum mechanics and molecular mechanics (QM/MM) approach where the reactive part is treated quantum mechanically while the remaining enzyme and solvent molecules are treated classically by using molecular mechanics.[5b,9] This appears to be a very promising approach to elucidate enzymatic reactions. However, the recent studies on NAD^+-dependent dehydrogenases with this hybrid QM/MM approach give contradicting results, e.g. in the order of which a hydride and a proton are transferred to the substrate from NADH and a histidine residue, respectively.[5b,9] Therefore, thorough investigations are needed before this method can be routinely used to elucidate enzymatic reaction mechanisms. Also, it is essential that the theoretical method is validated on simpler systems at a high level of theory before applying it to enzymatic reactions. Our interest here is therefore focused on one of the simplest NAD^+-dependent dehydrogenases, namely the formate dehydrogenase (FDH; EC 1.2.1.2),[11] and our purpose is to elucidate the mechanism of this reaction at a high level of theory in the gas phase and in solution.

Formate dehydrogenase catalyzes the oxidation of formate to carbon dioxide (Scheme 1). During the reaction, a C−H bond is broken at the same time as a new one is formed. X-ray

* To whom correspondence should be addressed. E-mail: tcbruice@bioorganic.ucsb.edu.

† Current address: DuPont Agricultural Products, Stine-Haskell Research Center, Newark, DE 19714.

(1) Walsh, C. *Enzymatic Reaction Mechanism*; W. H. Freeman and Company: San Francisco, CA, 1979. Blankenhorn, G. In *Pyridine-Nucleotide-Dependent Dehydrogenases*; Sund, H., Ed.; Walter de Gruyter: West Berlin, 1977; pp 185−205.

(2) (a) Wu, Y.-D.; Houk, K. N. *J. Am. Chem. Soc*. **1987**, *109*, 906. (b) Wu, Y.-D.; Houk, K. N. *J. Am. Chem. Soc*. **1987**, *109*, 2226. (c) Wu, Y.-D.; Houk, K. N. *J. Am. Chem. Soc*. **1991**, *113*, 2353. (d) Wu, Y.-D.; Houk, K. N. *J. Am. Chem. Soc*. **1993,** *58,* 2043. (e) Wu, Y.-D.; Lai, D. K. W.; Houk, K. N. *J. Am. Chem. Soc*. **1995**, *117*, 4100.

(3) Tapia, O.; Cardenas, R.; Andres, J.; Colonna-Cesari, F. *J. Am. Chem. Soc*. **1988**, *110*, 4046. Tapia, O.; Andres, J.; Cardenas, R. *Chem. Phys. Lett*. **1992**, *189*, 395. Andres, J.; Moliner, V.; Safont, V. S.; Domingo, L. R.; Picher, M. T. *J. Org. Chem*. **1996**, *61*, 7777. Andres, J.; Moliner, V.; Safont, V. S. *J. Phys. Org. Chem*. **1996**, *9*, 498. Andres, J.; Moliner, V.; Safont, V. S.; Domingo, L. R.; Picher, M. T.; Krechl, J. *Bioorg. Chem*. **1996**, *24*, 10.

(4) Wilkie, J.; Williams, I. H. *J. Am. Chem. Soc*. **1992**, *114*, 5423.

(5) (a) Cummins, P. L.; Gready, J. E. *J. Comput. Chem*. **1990**, *11*, 791. (b) Ranganathan, S.; Gready, J. E. *J. Phys. Chem. B* **1997**, *101*, 5614.

(6) (a) Almarsson, Ö.; Karaman, R.; Bruice, T. C. *J. Am. Chem. Soc*. **1992**, *114*, 8702. (b) Almarsson, Ö.; Bruice, T. C. *J. Am. Chem. Soc*. **1993**, *115*, 2125. (c) Olson, L. P.; Bruice, T. C. *Biochemistry* **1995**, *34*, 7335. (d) Olson, L. P.; Luo, J.; Almarsson, Ö.; Bruice, T. C. *Biochemistry* **1996**, *35*, 9782.

(7) Buck, H. M. *Recl. Trav. Chim. Pays-Bas* **1996**, *115*, 329.

(8) Mestres, J.; Duran, M.; Bertran, J. *Bioorg. Chem*. **1996**, *24*, 69.

(9) Cunningham, M. A.; Ho, L. L.; Nguyen, D. T.; Gillian, R. E.; Bash, P. A. *Biochemistry* **1997**, *36*, 4800.

(10) Li, H.; Goldstein, B. M. *J. Med. Chem*. **1992**, *35*, 3560.

(11) Popov, V. O.; Lamzin, V. S. *Biochem. J*. **1994**, *301*, 625.

S0002-7863(98)00733-1 CCC: $15.00
Published on Web 07/10/1998

Scheme 1

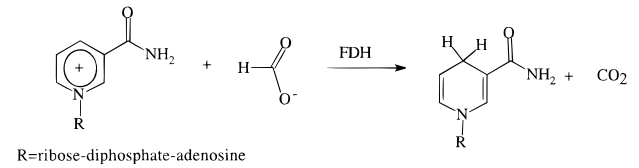

Scheme 2

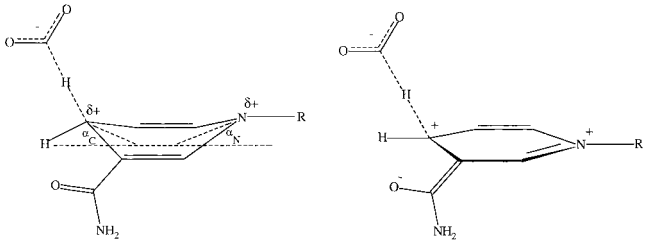

crystal structures have been solved for the apoenzyme and for the inhibited ternary complex of the holoenzyme with bound NAD^+ and an azide ion at resolutions of 2.05 and 1.80 Å, respectively (Brookhaven Protein Data Bank code 2NAD).[12] FDH is a dimeric protein with two identical subunits, each of which possesses NAD^+ and the substrate binding site.[12] It is known that FDH has an ordered kinetic mechanism in which NAD^+ binds first followed by formate binding.[13] One of the most important and disputed questions regarding NAD^+-dependent dehydrogenases concerns the conformation of the pyridine ring in the transition state.[11] Early on it was suggested that the pyridine ring is puckered in the transition state, and many earlier theoretical studies seemed to support this view.[2,6] Semiempirical AM1[14] calculations by Bruice and co-workers on lactate dehydrogenase models showed that ring puckering can reduce the activation barrier significantly.[6a,b] Indeed, earlier ^{15}N kinetic isotope investigation on FDH[15] did suggest a puckered ring in the transition state of the hydride transfer (**1** in Scheme 2). However, further studies with refined techniques concluded that the previously observed anomalous ^{15}N isotope effect for FDH is incorrect and the pyridine ring remains essentially planar during the hydride transfer (**2** in Scheme 2).[16]

Here we report a detailed investigation of the hydride transfer between formate and NAD^+ in the gas phase using high level *ab initio* molecular orbital theory to provide new insights into the conformation of the pyridine ring during the hydride transfer reaction and to gain knowledge of the energetics of the reaction. We also examine the reaction in the presence of a solvent.

Theoretical Procedure

In the present study molecular orbital theory methods are used. The PM3[17] Hamiltonian was used in the semiempirical calculations, and the calculations were done with AMPAC 5.[18] *Ab initio* molecular orbital calculations were carried out with the Gaussian 94 program.[19] Geometry optimizations were done at the HF/6-31+G(d,p) level of theory. Inclusion of diffuse functions is essential because anions are involved in the system, and having polarizable functions on the hydrogens is necessary because a hydrogen atom is the site of interest.[20] Most of the theoretical investigations pertaining to NAD^+-dependent dehydrogenases reported so far used either semiempirical quantum mechanical methods[3−8] such as AM1 and PM3 or *ab initio* quantum mechanical methods with a lower level of theory;[2,3,6,10] therefore, this study represents a great improvement in the model chemistry. NAD^+ and NADH were modeled by simple N-substituted nicotinamide and 1,4-dihydronicotinamide, respectively. Three N-substituents were examined, namely R = H (**a**), CH_3 (**b**), and CH_2OH (**c**). Transition states were located by using the Synchronous Transit-Guided Quasi-Newton (STQN) methods[21] available in the Gaussian 94 package.[19] All stationary points were identified as either a minimum (no imaginary frequencies) or a transition state (exactly one imaginary frequency) from vibrational analyses. For the found transition state using the hydroxyl methyl substituent (structure **8c**), a calculation of the Intrinsic Reaction Coordinate (IRC)[22] was carried out to confirm that the found transition state structure indeed corresponds to the hydride transfer. To further locate the ion-pair complex on the reactant side of the transition state, the resulting structure from the IRC was energy minimized to find the global minimum on the reactant side of the TS. Isotope effects were computed by including the zero-point vibrational energies resulting from the frequency calculations and using standard transition state theory.[23] Electron correlation effects were included through single-point calculations, applying the second-order Møller−Plesset perturbation[24] and a hybrid density functional theory[25] method (B3LYP).

Solvation effects on the hydride transfer reaction have been examined by using two different methods. The effect of acetonitrile solvation was studied with Tomasi's[26] polarizable continuum solvation model as implemented in the self-consistent reaction field (SCRF) part of Gaussian 94 (the self-consistent isodensity polarized continuum solvation (SCI-PCM)[27] option).[19] Due to the facts that geometry optimization in solution is very time consuming and that the SCI-PCM method with diffuse orbitals in the basis set has problems in converging when geometry optimization is sought (*vide infra*), the solvation calculations were run with a smaller basis set, 6-31G(d). Before doing so all structures were geometry optimized in the gas phase at the HF/6-31G(d) level of theory and the relative energies at the MP2/6-31G(d)//HF/6-31G(d) level of theory were computed. Only minor structural differences between the reactants, products, and transition state structures were found at the HF/6-31+G(d,p) and HF/6-31G(d) levels of theory, indicating that the smaller basis set can provide important information regarding the solvated reaction pathway. For the reaction in aqueous solution, the SM3-PM3[28] procedure, which is an extension of the PM3 method, was used; these calculations were performed with

(12) Lamzin, V. S.; Aleshin, A. E.; Strokopytov, B. V.; Yukhnevich, M. G.; Popov, V. O.; Harutyunyan, E. H.; Wilson, K. S. *Eur. J. Biochem.* **1992**, *206*, 441. Lamzin, V. S.; Dauter, Z.; Popov, V. O.; Harutyunyan, E. H.; Wilson, K. S. *J. Mol. Biol.* **1994**, *236*, 759.

(13) (a) Blanchard, J. S.; Cleland, W. W. *Biochemistry* **1980**, *19*, 3543. (b) Hermes, J. D.; Morrical, S. W.; O'Leary, M. H.; Cleland, C. C. *Biochemistry* **1984**, 23, 5479.

(14) Dewar, M. J. S.; Zoebisch, E. G.; Healy, E. F.; Stewart, J. J. P. *J. Am. Chem. Soc.* **1985**, *107*, 3902.

(15) Cook, P. F.; Oppenheimer, N. J.; Cleland, W. W. *Biochemistry* **1981**, *20*, 1817.

(16) Rotberg, N. S.; Cleland, W. W. *Biochemistry* **1991**, *30*, 4068.

(17) Stewart, J. J. P. *J. Comput. Chem.* **1989**, *10*, 209. Stewart, J. J. P. *J. Comput. Chem.* **1991**, *12*, 320.

(18) AMPAC 5.0, Semichem, 7128 Summit, Shawnee, KS 66216.

(19) Gaussian 94, Revision B.2, Frisch, M. J.; Trucks, G. W.; Schlegel, H. B.; Gill, P. M. W.; Johnson, B. G.; Robb, M. A.; Cheeseman, J. R.; Keith, T.; Petersson, G. A.; Montgomery, J. A.; Raghavachari, K.; Al-Laham, M. A.; Zakrzewski, V. G.; Ortiz, J. V.; Foresman, J. B.; Cioslowski, J.; Stefanov, B. B.; Nanayakkara, A.; Challacombe, M.; Peng, C. Y.; Ayala, P. Y.; Chen, W.; Wong, M. W.; Andres, J. L.; Replogle, E. S.; Gomperts, R.; Martin, R. L.; Fox, D. J.; Binkley, J. S.; Defrees, D. J.; Baker, J.; Stewart, J. J. P.; Head-Gordon, M.; Gonzalez, C.; Pople, J. A., Gaussian, Inc.: Pittsburgh, PA, 1995.

(20) Foresman, J. B.; Frisch, Æ. *Exploring Chemistry with Electronic structure Methods*, 2nd ed.; Gaussian, Inc.: Pittsburgh, PA, 1995−96.

(21) Peng, C.; Ayala, P. Y.; Schlegel, H. B.; Frisch, M. J. *J. Comput. Chem.* **1996**, 17, 49. Peng, C.; Schlegel, H. B. *Isr. J. Chem.* **1993**, *33*, 449.

(22) Gonzalez, C.; Schlegel, H. B. *J. Chem. Phys.* **1989**, *90*, 2174. Gonzalez, C.; Schlegel, H. B. *J. Phys. Chem.* **1990**, *94*, 5523.

(23) Hehre, W. J.; Radom, L.; Schleyer, P. v. R.; Pople, J. A. *Ab Initio Molecular Orbital Theory*; Wiley: New York, 1986.

(24) Møller, C.; Plesset, M. S. *Phys. Rev.* **1934**, *46*, 618.

(25) (a) Becke, A. D. *J. Chem. Phys.* **1993**, *98*, 5648. (b) Lee, C.; Yang, W.; Parr, R. G. *Phys. Rev. B* **1988**, *37*, 785.

(26) Tomasi, J.; Persico, M. *Chem. Rev.* **1994**, *94*, 2027.

(27) Wiberg, K. B.; Keith, T. A.; Frisch, M. J.; Murcko, M. *J. Phys. Chem.* **1995**, *99*, 9072. Wiberg, K. B.; Rablen, P. R.; Rush, D. J.; Keith, T. A. *J. Am. Chem. Soc.* **1995**, *117*, 4261. Wiberg, K. B., Castejon, H., Keith, T. A. *J. Comput. Chem.* **1996**, *17*, 185.

(28) Cramer, C. J.; Trular, D. G. *J. Comput.-Aided Mol. Des.* **1992**, *6*, 629.

Scheme 3

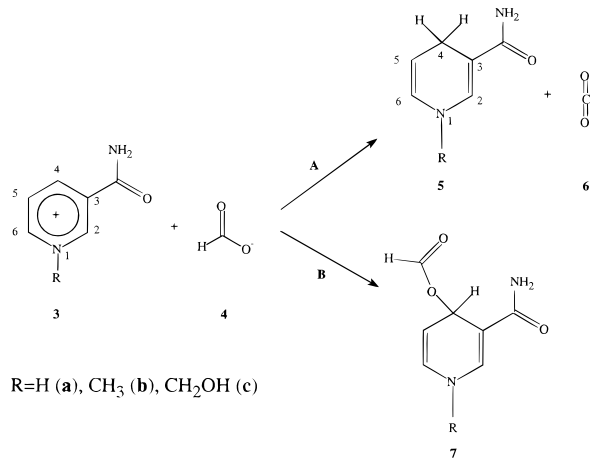

the AMPAC 5.0 program.[18] For the SM3-PM3 calculations, the gas-phase HF/6-31+G(d,p) optimized geometries were used, and single-point computations were undertaken.

Results and Discussion

Gas Phase. To simplify the computational effort, we used three smaller models for the N-substituent on the pyridine moiety in NAD^+, R being H (**a**), CH_3 (**b**), or CH_2OH (**c**) (Scheme 3). These three substituents were chosen to model the ribose-diphosphate-adenosine fragment bound to the nicotineamide ring of NAD^+ and NADH. Houk *et al.* have shown[2a,b] that the orientation of the ribosyl group relative to the nicotinamide ring is related to the stereospecificity of the dehydrogenase in question. Since we intend to investigate the influence of the N-substituent on the energetics and on the overall reaction pathway for the hydride transfer from formate to NAD^+, these three substituents are appropriate.

The reactions investigated are shown in Scheme 3. Apart from the normal hydride transfer reaction, charge separation can be annihilated by a simple nucleophilic addition of formate to NAD^+ (at either position 2, 4, or 6), resulting in a stable ester compound. Since the negative charge of formate is initially found on the two carboxylate oxygens, the formation of an ester, such as **7**, is likely to be the preferred reaction in the gas phase. Figure 1 gives the optimized structures for the species involved with R = CH_2OH. For comparison of the three models, computed structural data at the HF/6-31+G(d,p) level of theory are listed in Table 1 for NAD^+ (**3**), NADH (**5**), the transition state, TS (**8**), and the ester adduct (**7**).

The located transition states for hydride transfer look very similar for the models considered. The breaking C−H bond distance (H21−C22) is 1.245−1.248 Å for the three models, whereas the forming C−H bond (C4−H21) is slightly longer, around 1.53 Å. This indicates an early reactant-like transition state, which is consistent with the conclusions drawn from a model study of formate oxidation by 10-methylacridinium.[29] The transfer angle is also very similar in the three models, 155−163°, indicating an almost linear transition state for hydride transfer.[13] In **8**, the two C−O bonds of the formate moiety become shorter than in isolated formate, by about 0.01 and 0.04 Å, and the O−C−O angle has increased to 141.0°. Furthermore, the carboxamide group is in a *cis* conformation such that one amide hydrogen can form a hydrogen bond with one of the oxygen atoms of the formate moiety; the hydrogen bonding distance is 1.97 to 1.99 Å in the three models (Figure 1 and Table 1). Two possible transition state structures[11,15,16] have been proposed for the enzymatic reaction based on experimental findings, as was outlined in Scheme 2. On the basis of a study of kinetic isotope effects, Cleland *et al.*[16] speculated that the catalytic power of the enzyme may originate from enzymatic stabilization of a polar resonance isomer of NAD^+, leading to a polar transition state like **2**.[11] By inspection of the computed bond lengths of the transition state structures, **8**, it is seen that the C2−C3 bond is shorter in the TS than in NAD^+, where it is a partial double bond. The proposed enzymatic TS structure, **2**, thus becomes less likely in the gas phase, due to the fact that it has a single bond between C2 and C3. The bonding pattern found in the other proposed transition state structure, **1**, is consistent with the computed changes in bond lengths when proceeding from NAD^+ to the transition state on the reaction pathway. To further confirm that the located transition state is in fact the one corresponding to the hydride transfer reaction, an IRC[22]

Table 1. Important Structural Information for the Optimized Molecules in the Gas Phase at the HF/6-31+g(d,p) Level of Theory (Numbering Scheme According to Figure 1)[a]

	R = H (**a**)	R = CH_3 (**b**)	R = CH_2OH (**c**)
NAD^+ (**3**)			
N1−C2	1.330	1.328	1.336
C2−C3	1.381	1.385	1.381
C3−C4	1.388	1.383	1.386
C4−C5	1.396	1.395	1.393
C5−C6	1.367	1.366	1.368
C6−N1	1.343	1.346	1.346
C3−C11	1.514	1.514	1.513
C11−O12	1.196	1.197	1.197
C11−N13	1.342	1.342	1.343
TS (**8**)			
N1−C2	1.346	1.345	1.349
C2−C3	1.356	1.358	1.356
C3−C4	1.434	1.432	1.433
C4−C5	1.437	1.436	1.436
C5−C6	1.344	1.344	1.342
C6−N1	1.361	1.364	1.367
C3−C11	1.503	1.500	1.502
C11−O12	1.207	1.207	1.207
C11−N13	1.340	1.343	1.342
C4−H21	1.545	1.520	1.536
H21−C22	1.245	1.248	1.245
C22−O23/O24	1.211/1.194	1.209/1.194	1.210/1.194
∠O23−C22−O24	141	141	141
∠C4−H21−C22	155	164	158
H14−O23	1.967	1.991	1.978
NADH (**5**)			
N1−C2	1.363	1.366	1.372
C2−C3	1.337	1.338	1.334
C3−C4	1.520	1.517	1.517
C4−C5	1.512	1.509	1.509
C5−C6	1.323	1.324	1.322
C6−N1	1.389	1.394	1.398
C3−C11	1.483	1.483	1.485
C11−O12	1.210	1.210	1.209
C11−N13	1.356	1.357	1.356
ester (**7**)			
N1−C2	1.364	1.365	1.361
C2−C3	1.337	1.338	1.339
C3−C4	1.501	1.498	1.501
C4−C5	1.500	1.497	1.499
C5−C6	1.326	1.326	1.325
C6−N1	1.385	1.387	1.386
C3−C11	1.487	1.486	1.488
C11−O12	1.201	1.201	1.207
C11−N13	1.370	1.371	1.360
C4−O21	1.455	1.455	1.466
O21−C22	1.313	1.313	1.315

[a] Distances in Å and angles in deg.

(29) Hutchins, J. E. C.; Binder, D. A., Kreevoy, M. M. *Tetrahedron* **1986**, 993.

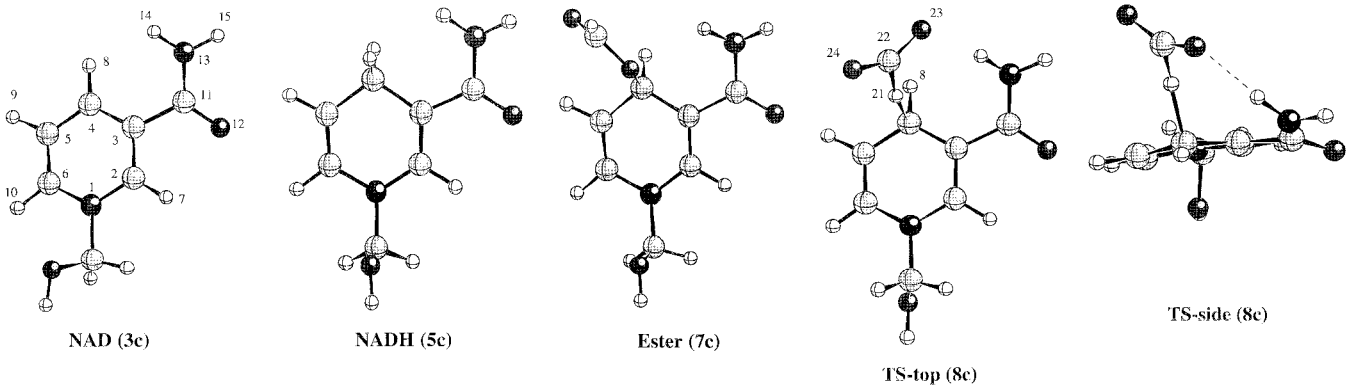

Figure 1. The optimized structures at the HF/6-31+G(d,p) level of theory. The structure of **8** is displayed in two different perspectives.

analysis was performed. The results confirmed the proposed mechanism, as the structures found on the two sides of the transition states eventually lead to the reactants and the products.

The optimized structures of the separated reactants and products are as expected, with NAD^+ and NADH both having a *cis*-oriented carboxamide group (note that there is a disagreement[10] in the literature of what *cis* and *trans* are; here we apply the notation mostly used, referring to *cis* as the conformer where the oxygen of the carboxamide group is *cis* to C2, see structures **3** and **5**). In NAD^+, the carboxamide group is rotated relative to the plane of the nicotinamide ring by 19°, whereas in NADH it is coplanar with the pyridine ring. Both findings are in excellent agreement with X-ray structural data[10] and earlier theoretical predictions.[2,6a,b,10]

On the basis of an experimentally large anomalous ^{15}N1 kinetic isotope effect in FDH catalyzed oxidation of formate to carbon dioxide, it was originally suggested that in the transition state for the hydride transfer the pyridine ring is in a boatlike conformation with N1 being pyramidal, **1**.[15] This conclusion seemed to agree with theoretical studies on related systems.[2c] However, in 1991, when the same experiment was repeated with a more sensitive technique, it was concluded that the ^{15}N isotope effect is normal and the pyridine ring remains planar during the hydride transfer process.[16] As seen in Figure 1, the pyridine ring has only a slight *quasi*-boatlike conformation in the calculated transition state structure, **8**, as C4 is bent toward the hydride by 7−9° (α_C), and N1 is bent out of the nicotinamide plane by 3−4° (α_N) (see **1** for the definition of α_C and α_N). These numbers are similar to what has been calculated by Houk *et al.*[2] for the hydride transfer between protonated pyridinium ion and 1,4-dihydropyridine and between protonated nicotinamide and 1,4-dihydronicotinamide. The computations also reveal that this transition state conformation gives rise to a planar nitrogen center, as the three bond angles around the nitrogen center add up to 359.5−360.0° for the three models evaluated. For NADH the sum of the three bond angles around N1 is lower, approximately 357°, indicating a slightly more pyramidal nitrogen center. The small change in pyramidalization of N1 going from NAD^+ to NADH can be concluded to take place after passing the TS on the reaction pathway. The emerging transition state structure from this analysis is thus slightly boatlike, though it retains the planar nitrogen center, and it is reactant-like.

Table 2 lists the calculated energetic data for the three applied models, **a**−**c**. Electron correlation effects were included by performing single-point calculations at the B3LYP/6-31+G(d,p)//HF/6-31+G(d,p) and MP2/6-31+G(d,p)//HF/6-31+G(d,p) levels of theory. An entry for semiempirical PM3 single-point calculations is also found in Table 2.

Figure 2 is a schematic drawing of the potential energy surface of the gas-phase reaction. All four methods (HF/6-31+G(d,p), MP2/6-31+G(d,p), B3LYP/6-31+G(d,p), and PM3) and all three models predict highly exothermic reactions for both hydride transfer and ester formation. Although the trends are similar, the calculated relative energies vary considerably among these four methods, with the MP2 and B3LYP results being very similar. It is thus evident that inclusion of electron correlation effects is important in this reaction. By comparison, the calculated energetic data for the semiempirical PM3 method resembles more the MP2 and B3LYP results than do the HF/6-31+G(d,p) results, which may reflect the fact that electron correlation effects were included in PM3 through the original parametrization.[17] At the MP2 level of theory, the reaction energy for the hydride transfer, reaction A, varies from −116.5 to −122.3 kcal/mol, whereas ester formation, reaction B, is exothermic by −104.4 to −110.3 kcal/mol in the gas phase for the three models used. All three models thermodynamically favor the formation of the products, CO_2 and NADH, over ester formation by approximately 12 kcal/mol.

To gain more insight into the reaction pathway, a search for the intermolecular ion-pair complex, IPC, between the two charged reactants was undertaken. The reactant structure resulting from the IRC calculation with R = CH_2OH was geometry optimized to give the local minimum on the potential energy curve corresponding to the intermolecular ion-pair complex, IPC, **9c**. The optimized structure of the ion-pair complex is depicted in Figure 3 for R = CH_2OH. For R = H and CH_3, IPCs were localized by adapting the geometry of **9c** and then minimizing the total energy. Important bond distances and angles are listed in Table 3 for **9a**−**c**. It is seen that all atoms are coplanar, with the two formate oxygens in close contacts to hydrogen donors of the NAD^+ fragment. Energetically, the formation of the IPC is favored by 101−105 kcal/mol for the three models studied at the MP2/6-31+G(d,p)//HF/6-31+G(d,p) level of theory. Again, from both an energetic and structural point of view the three N-substituents give very similar numbers and structures, which leads us to the conclusion that R = H is a good model for the reaction when one is studying the reaction pathway for hydride transfer from formate to NAD^+. Houk *et al.* have also used this as a model for NAD^+/NADH in similar studies of hydride transfer reactions, where focus has in fact been on the hydride transfer pathway.[2]

There is a considerable barrier to product formation from the ion-pair complex. A barrier height of approximately 18−19 kcal/mol is computed at the MP2/6-31+G(d,p)//HF/6-31+G(d,p) level of theory. The transition state for ester formation, **10c**, was found for R = CH_2OH. The structure is outlined in

Table 2. The Calculated Energies (in hartrees, 1 hartree = 627.5 kcal/mol) for the Gas-Phase Reactions[a]

compd	HF/6-31+G(d,p)	MP2/6-31+G(d,p)	B3LYP/6-31+G(d,p)	PM3
CO_2	−187.63879	−188.11218	−188.58750	−81.1
formate	−188.20969	−188.71613	−189.21888	−108.9
R = H (**a**)				
TS	−603.19432	−605.01755	−606.74211	−39.9
NAD^+	−414.87663	−416.16349	−417.37997	161.5
NADH	−415.65044	−416.96251	−418.20273	−5.2
ester	−603.25846	−605.05540	−606.76573	−76.2
R = CH_3 (**b**)				
TS	−642.22625	−644.19923	−646.05540	−41.4
NAD^+	−453.91496	−455.35029	−456.69905	158.6
NADH	−454.67950	−456.14002	−457.51297	−6.1
ester	−642.28754	−644.23275	−646.07601	−76.5
R = CH_2OH (**c**)				
TS	−717.08639	−719.23494	−721.27160	−79.9
NAD^+	−528.77322	−530.38605	−531.91470	119.1
NADH	−529.54178	−531.16706	−532.73284	−45.7
ester	−717.15286	−719.27572	−721.29962	−115.1

[a] The PM3 energy is heat of formation, measured in kcal/mol.

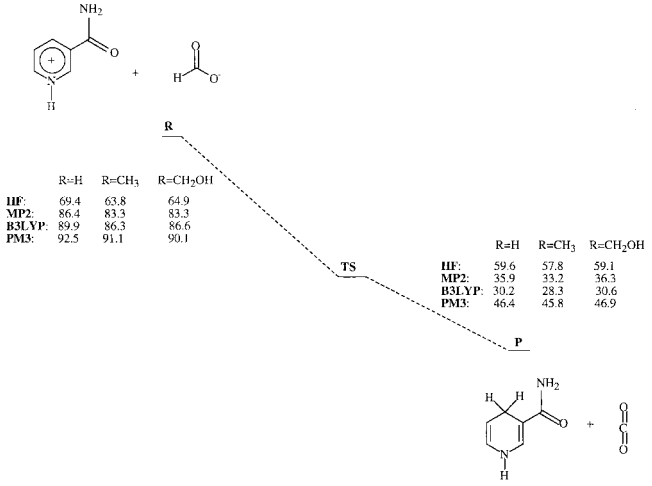

Figure 2. A schematic drawing of the calculated potential energy profile in the gas phase at different levels of theory. The MP2, B3LYP, and PM3 results are based on the HF/6-31+G(d,p) optimized geometries. Listed numbers refer to calculated energy differences (kcal/mol) between reactants and TS, and between TS and products.

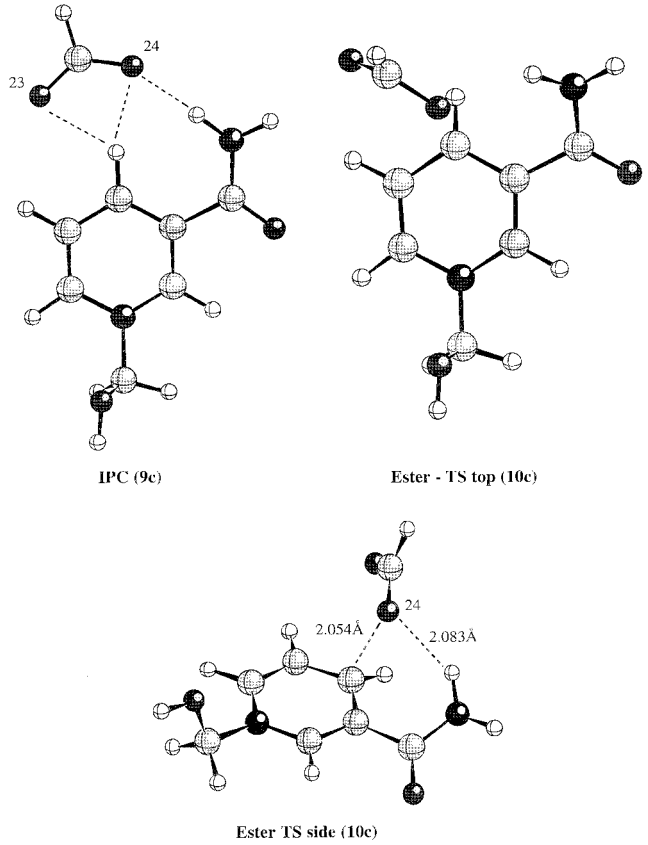

Figure 3. The optimized structures of the ion-pair complex, IPC, **9c**, and of the transition state for ester formation, **10c**, for R = CH_2OH at the HF/6-31+G(d,p) level of theory. The structure of **10c** is displayed in two perspectives.

Figure 3. Upon comparison of the structure of the TS for ester formation with the structure of the TS for hydride transfer, **8c**, the most striking difference is in the conformation of the pyridine ring. In **9c**, α_N is 0.8° compared to 4.2° in **8c**, whereas α_C is 3.5° in **9c** and 4.2° in **8c**, both indicating a more planar ring in **9c**. The difference most likely is due to the fact that more negative charge is located on the oxygens, thereby facilitating oxygen attack. Once the ion-pair complex has formed, it is much easier for it to rearrange to form the ester adduct, **7**, as the energy difference between the ester TS and IPC is computed to be only 1 kcal/mol at the MP2/6-31+G(d,p)//HF/6-31+G(d,p) level of theory. The emerging reaction profile is shown in Figure 4 for the part of the reaction pathway going from IPC to products or ester.

Kinetic Isotope Effects. Kinetic isotope effects have been used widely to probe the structure of transition states of chemical and enzymatic reactions.[30] Since kinetic isotope effects for formate oxidation by a model system, 10-methylacridinium,[29] and by formate dehydrogenase[11,16] are available, it would be of great interest to compare the experimentally measured values with those calculated from the gas phase *ab initio* transition state structure of the model reaction. The kinetic isotope effects were calculated according to the formula of eq 1 at 298.15 K.[31]

$$k_{\text{normal}}/k_{\text{isotope}} = \exp((\Delta G^{\ddagger}_{\text{isotope}} - \Delta G^{\ddagger}_{\text{normal}})/RT) \quad (1)$$

$$\Delta G^{\ddagger} = G_{\text{TS}} - G_{\text{reactant}}$$

The free energies were calculated using standard techniques[23]

(30) Melander, L. C. S.; Saunders: W. H., Jr. *Reaction Rates of Isotopic Molecules*; Wiley: New York, 1980. Jencks, W. P. *Catalysis in Chemistry and Enzymology*; McGraw-Hill: New York, 1969. Gandour, R. D.; Schowen, R. L. *Transition States of Biochemical Processes*; Plenum Press: New York, 1978.

(31) Glad, S. S.; Jensen, F. *J. Org. Chem.* **1997**, *62*, 253.

Table 3. Important Structural Information for the Ion-Pair Complex, **9**, Calculated at the HF/6-31+G(d) Level of Theory[a]

	R = H (**a**)	R = CH_3 (**b**)	R = CH_2OH (**c**)
N1−C2	1.333	1.332	1.334
C2−C3	1.376	1.379	1.376
C3−C4	1.389	1.385	1.387
C4−C5	1.400	1.399	1.399
C5−C6	1.361	1.361	1.360
C6−N1	1.350	1.353	1.354
C3−C11	1.513	1.513	1.512
C11−O12	1.210	1.211	1.211
C11−N13	1.326	1.326	1.326
H8−O23	2.178	2.176	2.175
H8−O24	1.999	2.016	2.019
O24−H14	1.856	1.855	1.851

[a] Distances in Å.

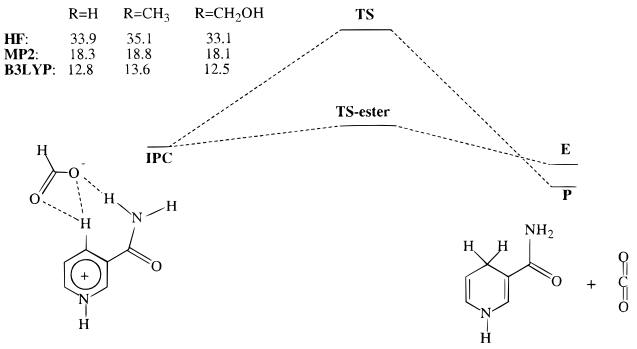

Figure 4. A schematic drawing of the potential energy profile from IPC to products at different levels of theory. The MP2 and B3LYP results are based on the HF/6-31+G(d,p) optimized geometries. The activation energy (kcal/mol) for the hydride transfer is shown for the three levels of theory considered.

and include the zero-point vibrational energies generated in the frequency analyses. It should be noted that the reported numbers are found with respect to the separated reactants and the transition state for R = CH_2OH. The calculated kinetic primary isotope effect for the transferring hydride, k_H/k_D, is 2.91 at the HF/6-31+G(d,p) level of theory. This is in good agreement with the experimental value of 2.1−3.1 for the enzymatic reaction[11,13] and 3.14 for the reaction with the NAD^+-model 10-methylacridinium.[29] Similarly, the calculated secondary kinetic isotope effect for ^{15}N1 gives a value of 1.0042, which is comparable to the experimental value of 1.004 ± 0.001 for hydride transfer from formate to an acetyl-substituted NAD^+-model fragment bound to the enzyme.[16] Clearly, these results are in good agreement with the experimental data. This calculated normal value of the secondary ^{15}N1 kinetic isotope effect further strengthens the proposal that the nitrogen center of the pyridine moiety remains planar in the transition state,[16] as it indicates that the hybridization of N1 is unchanged between the reactants and the transition state. Furthermore, the great similarity between the kinetic isotope effects calculated for the gas-phase reaction and the experimental kinetic isotope effect in the enzyme suggests that the transition state for formate oxidation in the enzyme closely resembles the gas-phase transition state structure. This is not surprising, since recent studies have shown that the transition state for an S_N2 displacement of a chloride anion from 1,2-dichlororethane by a carboxylate essentially remains the same, regardless of the environment.[32]

Solution. Formally, the reaction shown in Scheme 3 involves charge annihilation. Since both reactants are charged and both products are neutral, solvation is expected to have a dramatic effect on the reaction profile and the overall activation energy.

Table 4. Important Structural Information for the Optimized Molecules in This Study at the HF/6-31g(d) Level of Theory in the Gas Phase and in Acetonitrile (ϵ = 35.9), Using the SCI-PCM[27] Formalism[a]

	gas phase	acetonitrile
NAD^+		
N1−C2	1.330	1.329
C2−C3	1.380	1.377
C3−C4	1.388	1.391
C4−C5	1.395	1.390
C5−C6	1.366	1.370
C6−N1	1.330	1.337
C3−C11	1.514	1.506
C11−O12	1.194	1.208
C11−N13	1.334	1.336
TS		
N1−C2	1.345	1.346
C2−C3	1.355	1.355
C3−C4	1.433	1.451
C4−C5	1.436	1.445
C5−C6	1.342	1.340
C6−N1	1.345	1.364
C3−C11	1.503	1.488
C11−O12	1.206	1.211
C11−N13	1.339	1.348
C4−H21	1.578	1.395
H21−C22	1.261	1.310
C22−O23/O24	1.190/1.212	1.189/1.198
∠O23−C22−O24	141	143
∠C3−H21−C22	147	176
NADH		
N1−C2	1.365	1.355
C2−C3	1.334	1.340
C3−C4	1.519	1.521
C4−C5	1.511	1.512
C5−C6	1.320	1.321
C6−N1	1.365	1.391
C3−C11	1.482	1.476
C11−O12	1.206	1.220
C11−N13	1.362	1.348
ester		
N1−C2	1.364	1.354
C2−C3	1.335	1.342
C3−C4	1.500	1.498
C4−C5	1.499	1.497
C5−C6	1.323	1.326
C6−N1	1.386	1.380
C3−C11	1.486	1.482
C11−O12	1.199	1.212
C11−N13	1.374	1.357
C4−O21	1.454	1.467
O21−C22	1.313	1.306

[a] Distances in Å and angles in deg.

As mentioned above, geometry optimization with the self-consistent isodensity polarized continuum solvation model (SCI-PCM)[19] is very time consuming. It also has convergence problems when diffuse orbitals are included in the basis set. Therefore, the solvation calculations were performed at the HF/6-31G(d) level of theory with R = H (model **a**). Optimizations at the HF/6-31G(d) level of theory was carried out in the gas phase for R = H to see whether this basis set produces structures and energies similar to those at the HF/6-31+G(d,p) level of theory. NAD^+, NADH, CO_2, and formate were energy minimized and the transition state for hydride transfer was localized. All geometries (Table 4) are structurally very similar to those at the HF/6-31+G(d,p) level of theory. All bond distances

(32) Maulitz, A. H.; Lightstone, F. C.; Zheng, Y.-J.; Bruice, T. C. *Proc. Natl. Acad. Sci. U.S.A.* **1997**, *94*, 6591. Lightstone, F. C.; Zheng, Y.-J.; Maulitz, A. H.; Bruice, T. C. *Proc. Natl. Acad. Sci. U.S.A.* **1997**, *94*, 8417. Lightstone, F. C.; Zheng, Y.-J.; Bruice, T. C *J. Am. Chem. Soc*. **1998**, *120*, 5611.

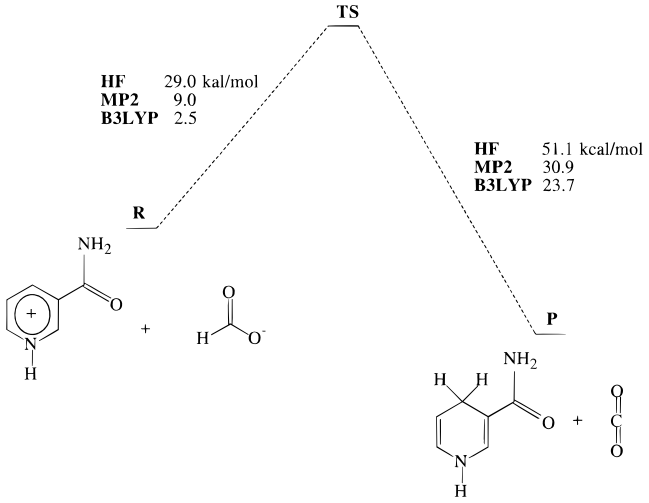

Figure 5. The calculated reaction energy profile in acetonitrile (ϵ = 35.9), using the SCI-PCM method at the HF/6-31G(p) level of theory. The MP2 and B3LYP results (kcal/mol) are based on the HF-SCRF/6-31G(d) optimized solution geometries.

Table 5. The Calculated Energies (in hartree, 1 hartree = 627.5 kcal/mol) for the Reaction in Acetonitrile, Model **a**, Using the SCI-PCM[27] Formalism[a]

compd	HF/6-31G(d)	MP2/6-31G(d)	B3LYP/6-31G(d)
CO_2	−187.63959	−188.10504	−188.58145
formate	−188.28449	−188.76449	−189.27496
TS	−603.19138	−604.93519	−606.72143
NAD^+	−414.95308	−416.18500	−417.45041
NADH	−415.63319	−416.87943	−418.17771
ester	−603.24410	−604.96496	−606.73910

[a] The electron-correlation entries are single-point calculations with the HF-SCRF/6-31G(d) optimized structures in acetonitrile (ϵ = 35.9).

differed by less than 0.005 Å, except the N−C bonds which differed by as much as 0.02 Å. For the TS, the largest structural differences are found around the transferring hydride. The 6-31G(d) basis set gives a smaller transfer angle (C4−H21−C22) of about 10°. Overall, the structural features of the transition state are maintained by using the 6-31G(d) basis set; the planar N1 center, the *quasi*-boat conformation of the pyridine ring, and the hydrogen bond between the *cis*-carboxamide arm and the formate oxygen are all present at the HF/6-31G(d) level of theory. Furthermore, it is found that the potential energy profile of the reaction at the HF/6-31G(d) level of theory closely resembles the HF curve of Figure 2. This indicates that calculations at the HF/6-31G(d) level of theory can provide important information on the solvated hydride transfer reaction.

Figure 5 displays the calculated reaction profile in acetonitrile (ϵ = 35.9) at the HF-SCRF/6-31G(d) level of theory. As expected, the shape of the potential energy surface changes dramatically in the presence of solvent. At the HF-SCRF/6-31G(d) level of theory the attempted optimization of IPC did not converge. A single-point calculation with the gas-phase structure of **9a** indicates that IPC in solution is of a significantly higher energy than the separated reactants and is therefore no longer the global minimum on the reactant side. At the MP2-SCRF/6-31G(d) level of theory, hydride transfer (reaction A) is still exothermic, but only by about 21.9 kcal/mol, while ester formation (reaction B) becomes almost thermoneutral (see Table 5). In acetonitrile there is an overall potential energy barrier toward oxidation of formate. The estimated height of the potential energy barrier is 9.0 kcal/mol (Figure 5), which is significantly lower than the barrier found in the gas phase when going from IPC via TS to the products. The SCI-PCM solvation method is very approximate, as it only evaluates electrostatic effects. Other effects, such as specific hydrogen bonding and cavity effects, are not accounted for in this model.[27] This calculated reaction barrier therefore presents a lower limit, as it is expected that hydrogen bonding interactions between solute and solvent will stabilize the separated charged reactants more than it does a polar transition state. It is also well-known that the MP2 level of theory stabilizes transition state structures too much, thereby underestimating reaction barriers.[2e]

The STQN method for transition state location was successful in locating the TS for hydride transfer in acetonitrile (ϵ = 35.9) with the 6-31G(d) basis set. The computed bond lengths and bond angles of the transition state are listed in column two of Table 4 together with the data for solvated NAD^+, NADH, and ester. The optimized structures of NAD^+, NADH, and the ester are all essentially unaffected by solvation in acetonitrile. On the other hand, the overall structure of the transition state in solution differs from the one found in the gas phase at the HF/6-31G(d) level of theory. The most notable differences are found in the positioning of the transition state along the reaction coordinate. The position of the hydride in the solvated transition state is closer to C4 and further away from the formate carbon, C22, than in the gas-phase TS. The optimized bond distance for H21−C22 increases from 1.261 Å to 1.310 Å whereas the C4−H21 bond distance decreases from 1.518 Å to 1.395 Å upon moving from the gas phase to acetontrile. The transfer angle is estimated to be 175°, which is in good agreement with Cleland and co-workers' proposal of a linear transition state in the enzymatic reaction[13,15,16] but about 20−30° larger than that found in the gas-phase transition state. All other computed parameters for the transition state of the reaction in solution are consistent with a later and slightly more product-like transition state than found in the gas-phase reaction. In light of this finding, it is notable that N1 retains its planar binding geometry in the TS also in acetonitrile; the bonding angles around N1 add up to 359.8°. Overall, the computations suggest that the conformation of the pyridine moiety of NAD^+ in the transition state is *quasi*-boatlike (α_C = 8.9° and α_N = 3.7° in acetonitrile) with a planar N1 center in acetonitrile as well as in the gas phase. The more product-like transition state in solution is in agreement with the Hammond postulate,[33] as the difference between the solution energies of reactants and products is smaller than the difference between the gas-phase energies of IPC and products.

It has been shown previously[34] that a model compound of NAD^+ (1-benzyl-3-carbamoylpyridinium perchlorate) can oxidize formate in dry acetonitrile in the presence of 18-crown-6 ether to carbon dioxide and 1-benzyl-3-carbamoyl-1,4-dihydropyridine. The other minor product (∼20%) is 1-benzyl-3-carbamoyl-1,6-dihydropyridine. However, there is no evidence that the reaction actually occurs through a hydride transfer process. As discussed above, since the negative charge is on the two carboxyl oxygens in formate, direct nucleophilic addition of formate to NAD^+ at either position 4 or 6 is likely to be preferred. The 1,4-dihydropyridine and 1,6-dihydropyridine are probably formed by decarboxylation of the ester intermediates resulting from nucleophilic addition of formate to NAD^+.[34] A single-point calculation with the gas phase TS structure for ester formation in acetonitrile indicate that only a very small (HF-SCRF/6-31G(d)//HF/6-31+G(d,p)) or no (MP2-SCRF/6-31G(d)//HF/6-31+G(d,p)) barrier at all is found for ester formation

(33) Hammond, G. S. *J. Am. Chem. Soc*. **1955**, *77*, 334. Thornton, E. R. *J. Am. Chem. Soc*. **1967**, *89*, 2915.
(34) Ohnishi, Y.; Tanimoto, S. *Tetrahedron Lett*. **1977**, *18*, 1909.

Table 6. Calculated Heat of Formation Energies for the Reaction in Water at the SM3-PM3 Level of Theory[a]

compd	R = H (**a**)	R = CH_3 (**b**)	R = CH_2OH (**c**)
CO_2	−87.3	−87.3	−87.3
formate	−184.9	−184.9	−184.9
TS	−74.4	−66.1	−109.8
NAD^+	88.7	98.1	54.0
NADH	−22.8	−19.2	−64.2
ester	−100.4	−95.4	−136.4
IPC	−91.4	−80.6	−124.4

[a] All entries are single-point calculations, using the HF/6-31+g(d,p) optimized structures from the gas phase. SM3-PM3 energies are in kcal/mol.

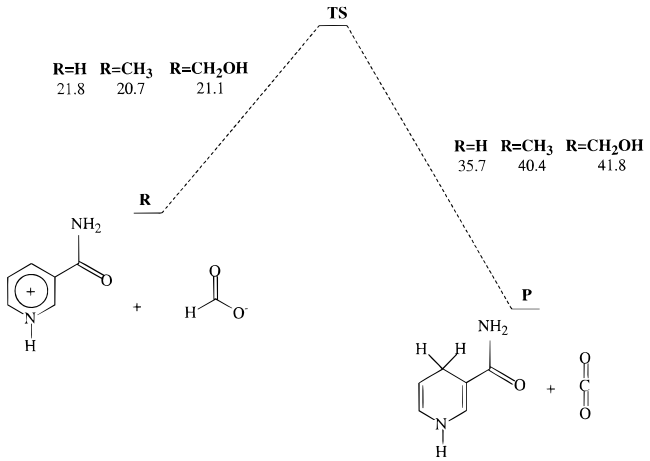

Figure 6. The calculated reaction energy profile in aqueous solution, using the SM3-PM3 solvation model based on the HF/6-31+G(d,p) geometries. The numbers are energy differences (kcal/mol) for the three substituents.

in acetonitrile. The calculations thus support the proposal that the ester adduct is the kinetic product, whereas CO_2 and NADH are thermodynamically favored.

We also examined the reaction between formate and NAD^+ in aqueous solution using the SM3-PM3 semiempirical method.[28] The parametrization of SM3-PM3 does account for hydrogen bonding between solute and solvent, so the energies produced with this method are more realistic, within the accuracy of the PM3 method, than the SCI-PCM energies. The calculated relative energies are shown in Table 6 for the three models studied. The SM3-PM3 calculations also show that the intermolecular ion-pair complex, **9**, is no longer a global minimum on the reactant side. Figure 6 displays the potential energy profile for the three models. Again, there is a significant potential barrier, approximately 21 kcal/mol, for hydride transfer in solution, whereas the barrier for ester formation is 17 kcal/mol at the SM3-PM3 level of theory. This is consistent with the experimentally known fact that at room temperature, 1-benzyl-3-carboamoylpyridinium does not react with formate in aqueous solution,[34] and this is also expected from a theoretical point of view because water solvates the charged reactants much better than acetonitrile does, thereby disfavoring their reaction to a neutral substrate.

Conclusions and Implications for the Enzymatic Reaction

One of the most important questions in NAD^+-dependent dehydrogenases regards the conformation of the pyridine ring in the transition state. To examine the conformation of the pyridine ring in the hydride transfer between formate and NAD^+, high level *ab initio* molecular orbital calculations were performed. According to the present study, neither of the two proposed transition state structures in Scheme 2 are correct, as the computations reveal a transition state, where the pyridine ring has a *quasi*-boat conformation with a *planar* nitrogen center. The finding of a planar nitrogen center agrees with the conclusion reached by Cleland and co-workers[16] based on ^{15}N isotope investigation of FDH-catalyzed oxidation of formate to carbon dioxide. The good agreement between the calculated kinetic isotope effects for the reaction in the gas phase and the experimental isotope effects in model systems[29] and in the enzyme suggests that the general structure of the transition state does not change significantly when the environment is changed. This is in agreement with recent findings for the S_N2 displacement of a chloride anion of dichloroethane by aspartate in dehalogenases.[32] It is possible that the conformation of the pyridine ring can be affected by the enzymatic environment, and that for different dehydrogenases the conformation of the pyridine ring could be different. Further studies of hydride transfer transition states in the active site of dehydrogenases could shed more light on these matters.

Scheme 4

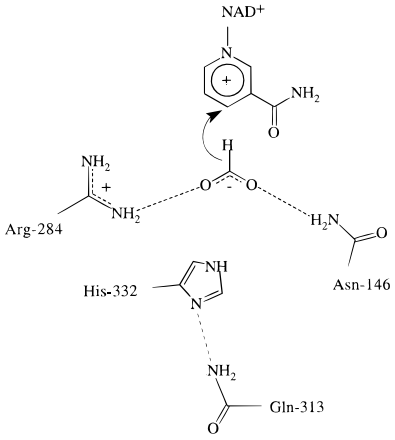

On the basis of the above discussion, it has become clear that the reaction between formate and NAD^+ in a vacuum is energetically extremely favorable; however, the reaction forms an ester adduct by nucleophilic addition, instead of 1,4-dihydropyridine *via* hydride transfer. Due to severe solvation effects of the charged reactants, there is a significant potential energy barrier for the hydride transfer reaction in solution; even in acetonitrile, the formation of the ester adduct seems to be favored. The obstacle the enzyme must overcome is to prevent this side reaction (the formation of ester adduct) from happening. Thus, the enzyme must orient the formate correctly in the active site to keep the carboxylate oxygens away from the C4 position of NAD^+.

Although the crystal structure of FDH with bound NAD^+ and formate is not available, the crystal structure of FDH isolated from *Pseudomonas sp. 101* with bound NAD^+ and azide (N_3^-) is known.[12] Azide is isoelectronic with the oxidation product, CO_2, and both molecules are linear. It is reasonable to expect that formate binds similarly to azide in the ternary complex with NAD^+ and the enzyme. Scheme 4 depicts the binding environment of formate in the active site as suggested by Popov and co-workers.[11] Indeed, in the active site, Arg-284 and Asn-146 are positioned to bind formate appropriately for hydride transfer through electrostatic and hydrogen bonding interactions. Mutagenesis studies have confirmed the importance of Arg-284, since the alanine mutant of Arg-284 is inactive.[11] The Arg-284 Gln mutant shows only about 1.5% of the wild-type enzyme activity and a 25-fold decrease in substrate affinity, suggesting the importance of Arg-284 in substrate binding and in the actual

catalytic step.[11] Recent mutagenesis studies[35] have additionally revealed that His-332 is important for substrate binding. We have started molecular dynamics simulations of the enzyme−substrate complex in order to examine the binding of formate in the active site and the role of the three important amino acid residues.

Scheme 4 also reveals that in the enzyme the carboxamide arm cannot stabilize formate during hydride transfer as it is found in the *trans* conformation.[12] At the HF/6-31+G(d,p) level of theory the *trans* conformation is only 1.6 kcal/mol higher in energy than the favored *cis* conformation, and the barrier for rotation is 4 kcal/mol at the 6-31G(d) level of theory.[2c] This change in preferred orientation of the carboxamide group upon binding at the enzyme active site is, thus, a low-energy conformational change. Theoretical studies have shown that C4 has more carbonium ion character in the *trans* conformer than in the *cis* conformer of NAD^+ in the gas phase.[2,10] The molecular dynamics simulations will, hopefully, be helpful in elucidating the importance of the conformation of NAD^+ in the enzyme substrate complex as well as in the transition state.[32c]

The present analysis suggests that the role of the enzyme is to align formate and NAD^+ in a reactive intermolecular conformation. In other words, the enzyme stabilizes the NAC (Near Attack Conformer) in the enzyme−substrate complex.[36] According to the solution calculations, solvation of the reactants can impose a significant barrier on the hydride transfer. Paradoxically, it can be expected that the strong interaction between formate and Arg-284 and Asn-146 presumably found in the active site of formate dehydrogenase could also lead to such a barrier for the hydride transfer, which may be the reason FDH is a relatively slow enzyme compared to other NAD^+-dependent dehydrogenases.

Acknowledgment. This work was supported by a grant from the National Science Foundation. We also appreciate the National Center for Supercomputing Applications (Urbana−Champaign, IL) for allocation of computing resources (Grant No. CHE980016N). B.S. thanks the Danish Natural Science Research Foundation for providing a postdoctoral fellowship.

JA9807338

(35) Tishkov, V. I.; Matorin, A. D.; Rojkova, A. M.; Fedorchuk, V. V.; Savitsky, P. A.; Dementieva, L. A.; Lamzin, V. S.; Mezentzev, A. V.; Popov, V. O. *FEBS Lett*. **1996**, *390*, 104.

(36) Lightstone, F. C.; Bruice, T. C. *J. Am. Chem. Soc*. **1996**, *118*, 2595; **1997**, *119*, 9103.